CARBON 50 (2012) 3708–3716

Available at www.sciencedirect.com

SciVerse ScienceDirect

journal homepage: www.elsevier.com/locate/carbon

The mechanical responses of tilted and non-tilted grain boundaries in graphene

Young In Jhon [a], Shou-En Zhu [a,b], Jong-Hyun Ahn [a], Myung S. Jhon [a,c,*]

[a] School of Advanced Materials Science and Engineering, Sungkyunkwan University, Suwon 440-746, Republic of Korea

[b] Micro & Nano Engineering Lab, Department of Precision and Microsystems Engineering, TU Delft, Mekelweg 2, 2628 CD Delft, The Netherlands

[c] Department of Chemical Engineering and Data Storage Systems Center, Carnegie Mellon University, Pittsburgh, PA 15213, USA

ARTICLE INFO

Article history:
Received 12 June 2011
Accepted 27 March 2012
Available online 3 April 2012

ABSTRACT

Various mechanical characteristics of tilted and non-tilted grain boundaries in graphene were investigated under tension and compression in directions perpendicular and parallel to the grain boundaries using molecular dynamics simulation. In contrast to the non-tilted grain boundary and the pristine graphene, the mechanical response of tilted grain boundary was observed to be quite unique under perpendicular tension, exhibiting distinct crack propagation prior to tensile failure and the subsequent pattern of incomplete fracture. These features are manifested as a remarkable decrease in the slope and a rugged pattern in the stress–strain curves. The characteristic of incomplete fracture was striking especially for large misorientation angles with formation of long monoatomic carbon chains, suggesting a methodology for feasible production of the monoatomic carbon chains that have been difficult to synthesize and extract. Under perpendicular compression, the folding of the sheet occurred consistently along grain boundaries during the entire process, indicating a tunable folding, while the folding line wandered extensively for pristine graphene. Under parallel compression, we found that folding along grain boundaries disturbed the bending of the graphene substantially for intrinsic reinforcement.

1. Introduction

Graphene, a single atomic carbon film with hexagonal sp^2 covalently bonded crystal structure, has opened an avenue for research opportunities to exploit its elegant properties, such as ultrahigh electronic mobility [1,2], superior thermal conductivity [3,4], and excellent mechanical strength with exceptional stretchability [5–7]. These extraordinary properties in the defect free network can be obtained easily, due to high formation energies of defects and strong bonding of carbon atoms [8]. Recently, breakthroughs have occurred in the synthesis of large-scale single layered graphene film based on the chemical vapor deposition (CVD) technique, bringing it much closer to practical application [9,10]. This large-scale metallic catalyst based process, however, has intrinsically generated the polycrystalline form of graphene, owing to crystal imperfections of substrate material and kinetic influence in the growth process [11–14] and grain boundaries have become one of the most dominating intrinsic defects. In contrast to any other material, graphene is unique in that it can host lattice defects through the reconstruction of atomic arrangement, forming non-hexagonal rings. The simplest defects include the Stone Thrower Wales (STW) defect [15,16], which does not involve any removed or added atoms, and single vacancy [17,18] undergoing a Jahn–Teller distortion which leads to the saturation of two of the three dangling bonds toward the miss-

* *Corresponding author at*: Department of Chemical Engineering and Data Storage Systems Center, Carnegie Mellon University, Pittsburgh, PA 15213, USA. Fax: +1 412 268 7139.
E-mail address: mj3a@andrew.cmu.edu (M.S. Jhon).

0008-6223/$ - see front matter
http://dx.doi.org/10.1016/j.carbon.2012.03.044

ing atom. Foreign atoms can also be incorporated into graphene as substitutional impurities replacing one or two carbon atoms [19]. While these are point defects, the grain boundary is a one dimensional defect [20] and such a line defect can significantly influence the properties of a two-dimensional material. As a consequence, the role of grain boundaries is critical in graphene and it is believed that their intentional introduction and manipulation would be significant and play a crucial role in the development of graphene technology. Considerable efforts have been made to characterize grain boundaries in graphene [21–26], but a majority of the research has been dedicated to their electronic properties, while the mechanical properties in the presence of grain boundaries have remained elusive and are not fully understood yet.

To systemically address this issue, we investigated mechanical response when graphene is elongated or compressed in directions perpendicular or parallel to grain boundaries which are denoted by filled and open arrows, respectively, for the elongation process in Fig. 1(a). Mismatched zigzag-oriented (tilted) and perfectly matched armchair-oriented (non-tilted) graphene sheets [21,22] were examined, and their representative structures were depicted in Fig. 1. For tilted grain boundaries, we examined six cases by varying the misorientation angle (θ in Fig. 1(a)), and corresponding systems are denoted by T_i (i = 1–6, sequentially numbered in a descending order of the misorientation angle, i.e., 21.10°, 12.87°, 9.26°, 7.23°, 5.93°, and 5.03°). Pristine and perfectly matched armchair-oriented (non-tilted, that is, θ equals 0°) graphene sheets were denoted as PR and TZ, respectively. Molecular dynamics simulations were performed to investigate the mechanical characteristics of these systems. For this, optimized structures were obtained first at 298 K using NPT simulation followed by NVT simulation. The systems were then elongated or compressed uniaxially in direction perpendicular or parallel to grain boundaries from these relaxed structures. Compression was simulated by bending the graphene sheets through a reduction of box size in the uniaxial direction rather than fully compressing the sheets. As a consequence, the compression strain hereafter implies a normalized relative change in box size rather than actual graphene size.

2. Computational methods

The T_i systems were constructed to meet the periodic boundary condition by embedding two directionally opposite tilted grain boundaries to a pristine graphene (see Fig. S1). Detailed information on the systems is described in Table S1.

The cut-off parameter is set to be 2.0 Å in order to avoid spuriously high bond forces and unphysical results near the fracture region. This value has been tacitly used in previous research to study mechanical properties of graphene [6,27].

In an alternative approach, the value of 1.92 Å has been used to obtain a better quantitative agreement with experimental data for hydrogenated graphene and yielded success-

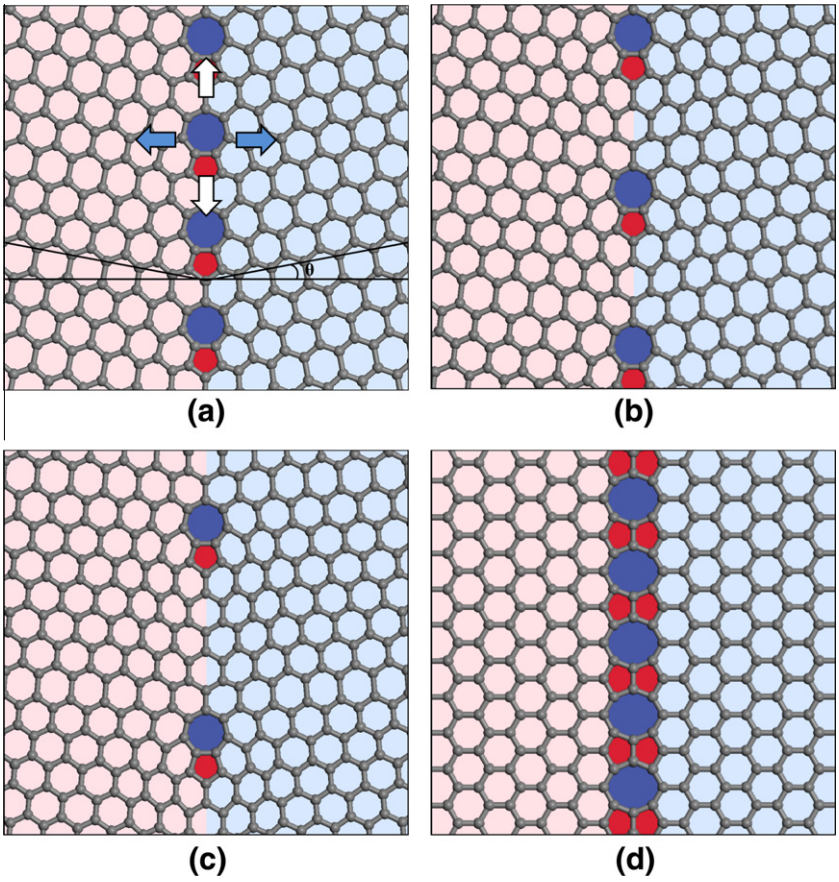

Fig. 1 – The structures of grain boundaries (a)–(c) in mismatched zigzag-oriented graphene sheets (T_1, T_2, and T_3 systems, respectively) and (d) perfectly matched armchair-oriented graphene sheet (TZ system).

ful results on graphene characteristics [28]. However, it may cause a certain spurious consequence in non-hydrogenerated graphene, as indicated by a persistent strength of 20 GPa even after tensile failure of the pristine graphene [28]. The error in employing the latter value was also observed in our test simulation where elongational behavior of the T_2 system was investigated using both quantum mechanical calculation using the DMol3 package [29] and molecular mechanics calculation. A 0.5% strain was applied between consecutive stages by scaling all atomic coordinates accordingly, and geometric optimization (corresponding to the case of zero temperature) was subsequently performed at each stage. In the quantum mechanical calculation, a crack was created under an approximate strain of 0.1 and it rapidly propagated along the grain boundary during subsequent stages, resulting in tensile failure as shown in Fig. 2(a) and (b). In the molecular mechanics calculation, a crack was also created under a similar value of strain for both cut-off parameters however, compared to that of quantum mechanical calculation, a critical difference was observed in the case of 1.92 Å where graphene did not undergo tensile failure even under the strain of 0.3 implying an over-approximation of bond strength, while it exhibited similar fracture behavior in the case of 2.0 Å as shown in Fig. 2(c)–(f). Hence, it was surmised that the selection of 2.0 Å as cut-off parameter should be more suitable to our study in which graphene is composed of carbon atoms bonded with sp^2 orbitals. The detailed computational condition and further results for this examination are given in Supplementary data.

Molecular dynamics simulations were performed using the software package LAMMPS [30] with the adaptive intermolecular reactive empirical bond order (AIREBO) potential [31] and a time step of 1.0 fs. To obtain optimized structures, the NPT simulation was first performed for 200,000 steps in which optimized volume size of the simulation system was determined by averaging the final 100,000 steps. Based on this box size, NVT simulation was performed consecutively for 100,000 steps. Finally the system was elongated or compressed uniaxially from the relaxed structures with a fixed lateral directional length. The strain rate was set to 0.5 ns^{-1} and 2000 steps were taken at each deformation point and, accordingly, 0.1% strain was applied to the system between two consecutive points. Non-equilibrium molecular dynamics (NEMD) simulations of a continuously strained system were carried out in which SLLOD equations of motion coupled to a Nose/Hoover thermostat were employed [32].

For the calculation of energy density in Section 3.4, an effective area of the graphene sheet was estimated using the horizontal and vertical lengths of graphene instead of simulation box dimensions as shown in Table S1.

3. Results and discussion

3.1. *Elongation parallel and perpendicular to grain boundaries*

When graphene was elongated parallel to the grain boundaries, our simulation indicated that it can sustain consider-

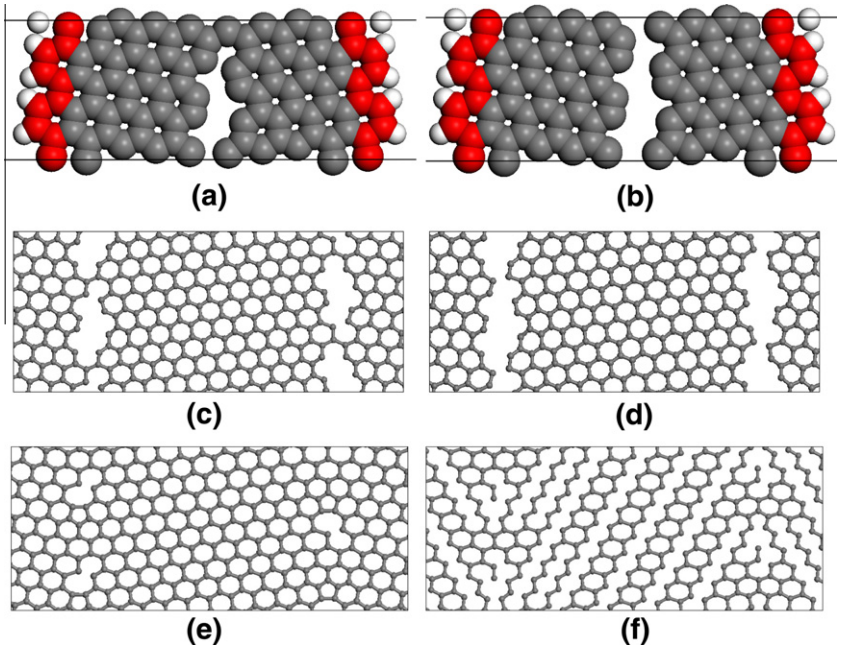

Fig. 2 – The structures during tensile process (a) and (b) obtained from quantum mechanical calculation at strain of 0.115 and 0.120, respectively, (c) and (d) obtained from molecular mechanics calculation at strain of 0.115 and 0.120 using cut-off parameter of 2.0 Å, respectively, and (e) and (f) obtained from molecular mechanics calculation at strain of 0.115 and 0.300 using cut-off parameter of 1.92 Å, respectively. White, gray, and red colors denote hydrogen, carbon, and positionally fixed carbon atoms respectively in (a) and (b). (For interpretation of the references to color in this figure legend, the reader is referred to the web version of this article.)

able amount of tensile strength compared to pristine graphene, which coincides with Grantab et al.'s study [25]. Specifically, the T_1 system exhibited the largest tensile strength among the tilted grain boundary systems and TZ was the strongest in all of the systems (Fig. 3). On the contrary, elongation perpendicular to the grain boundaries yielded much less tensile strength than pristine graphene. For tilted grain boundary systems, the tensile strength decreased as the misorientation angle decreased, which agrees well with the previous report [25] where this counterintuitive trend was explained based on initial strained condition of the weakest bonds in tilted grain boundaries.

Noticeably, our simulation also indicated that the fracture of graphene with tilted grain boundaries is much different than pristine graphene. It exhibited a distinct incomplete fracture behavior for a long period of time, especially for T_i ($i = 1–3$) systems, forming rugged tails after a tensile failure in stress–strain plots (Fig. 3). It is also notable that the slope of stress–strain curve decreased remarkably prior to the stage of tensile failure for T_2 and T_3 systems in contrast to pristine graphene.

3.2. *Structural analysis on elongation perpendicular to tilted grain boundaries*

To elucidate the mechanism of this extraordinary phenomenon, we performed in-depth investigation on the structural change of T_2 and T_3 systems during the elongation as shown in Figs. 4 and 5 where some critical stages in stress–strain plots of T_2 and T_3 systems are matched with their corresponding structures.

The origin of this unusual behavior occurring prior to the tensile failure coincided exactly with the stage at which the first bond breaking occurred. This took place at the heptagon in heptagon–pentagon pairs (Fig. 4(a)), which is consistent with the fact that heptagon bonds are the most strained in graphene as illustrated in a previous study [25] and our quantum mechanical calculation based on density functional theory (Fig. S2(c)).

Once the bonds had been broken at the heptagon, the crack began to propagate to other parts such as pentagonal or hexagonal regions as demonstrated in Fig. 4(b)–(d). A tensile failure of graphene occurred through a rapid growth of preexisting cracks accompanied by the newly created voids as shown in Fig. 4(e).

During the crack propagation, the stress required for elongation may be alleviated and it is expressed as a rapid decrease of slope in the stress–strain plots (Fig. 5). This pattern did not appear in the case of the largest misorientation angle (T_1), however, as the distance for crack propagation is very short and the crack propagation would be completed rapidly (Fig. 3(a) and Supplementary Movie 1). The T_4 system showed an absence of this pattern, displaying a complicated behavior (Fig. S5(b)).

As mentioned before, tilted grain boundaries did not result in complete fracture immediately even after the quasi tensile failure of the graphene. Instead, it induced long-lasting stringy connections between the two separated parts accompanied by large persistent strength, forming rugged tails in stress–strain plots (Fig. 5).

This phenomenon was striking, especially for large misorientational angles like T_i ($i = 1–3$) systems. The existence of such a string, termed as a monatomic carbon chain (MACC), was also discovered in the experiments in MWCNT. In addition, relevant theoretical investigations have been performed as well where its importance in micro-and nanoelectrome-

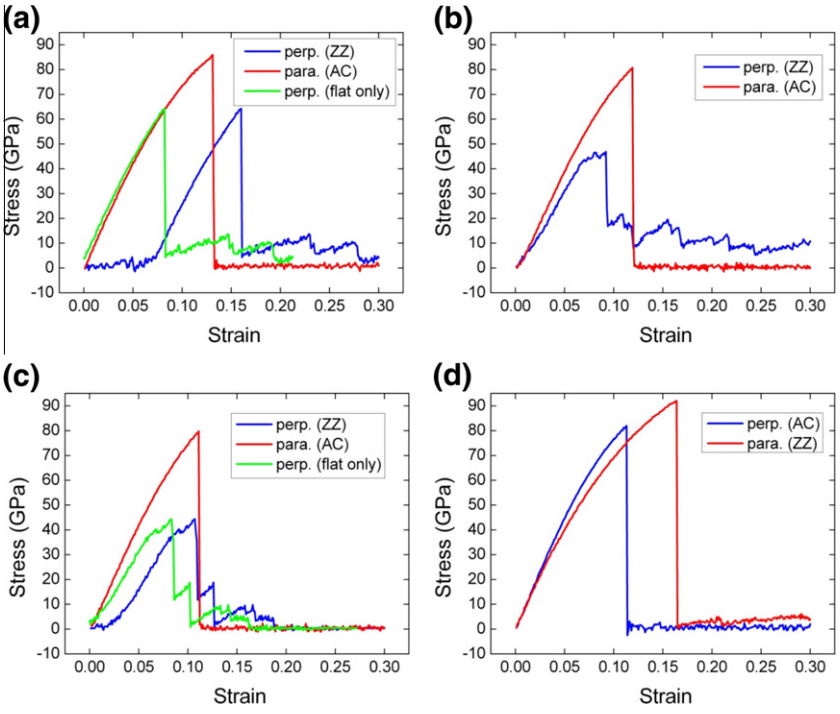

Fig. 3 – The stress–strain plots of (a)–(c) T_1, T_2, and T_3 systems, respectively and (d) TZ system, under tension perpendicular (perp.) and parallel (para.) to grain boundaries. ZZ and AC stand for zigzag and armchair directions, respectively.

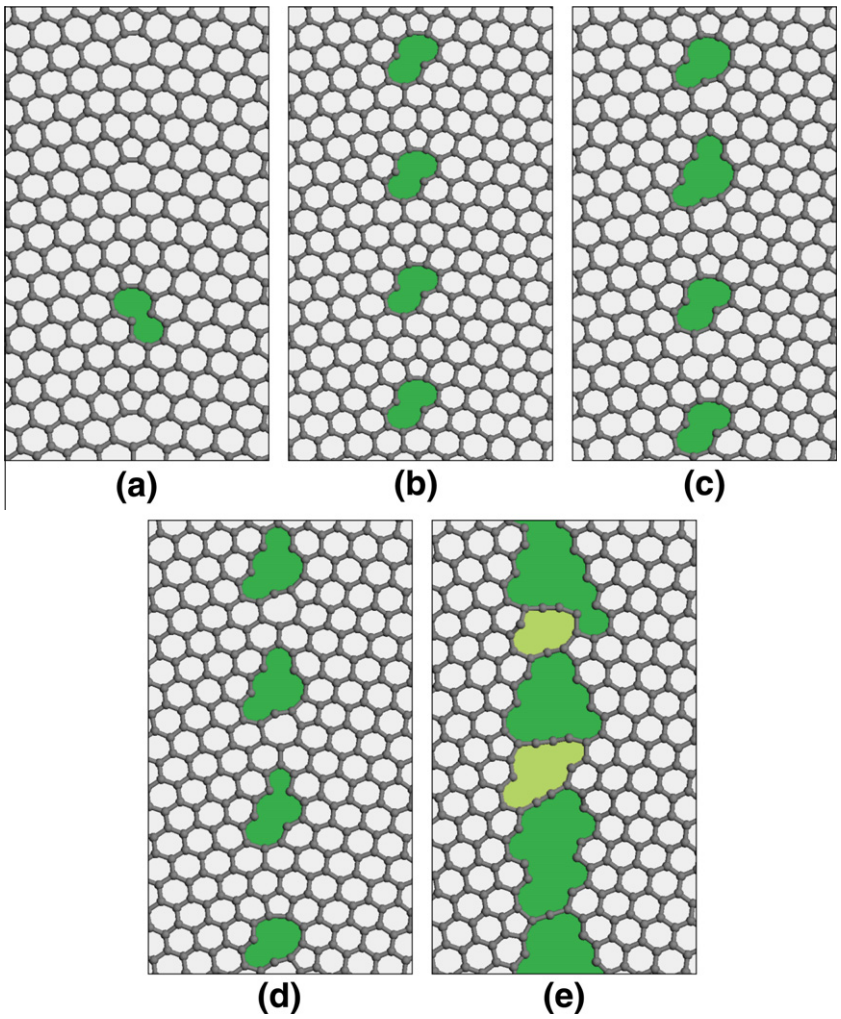

Fig. 4 – (a)–(e) Illustrative structures of T_2 system corresponding to A–E in Fig. 5(a), respectively. Green denotes crack regions present during crack propagation and florescent denotes void regions newly created at the stage of tensile failure. (For interpretation of the references to color in this figure legend, the reader is referred to the web version of this article.)

chanical systems (M/NEMS) was indicated [33–35]. Recently, fabrication of carbon atomic chains from graphene was also achieved by controlled electron irradiation in a transmission electron microscope, and these experiments demonstrated stability of chains with lengths of a few nanometers, setting the stage for a new methodology to produce chain-like structures bridged between graphene nanoribbons (GNRs) [36,37]. Furthermore, very recently, its use in the electronic switching was theoretically suggested when it is bridged between GNRs and structurally modified at the terminal edge under uniaxial strain [38]. MACC is known as carbyne or linear acetylenic carbon in chemistry, and it has been the subject of considerable debate, as a hypothetical carbon allotrope, in the scientific community [39,40]. In contrast to other carbon allotropes such as diamond, fullerene, and graphite, carbyne is a one-dimensional infinite chain molecule that entirely consists of sp-hybridized carbon atoms and it is characterized by extremely high physical fragility and reactivity, which has thwarted the attempts to isolate and fully study it. In this regard, it is important to investigate the potential of synthesizing and extracting MACC by mechanical elongation of graphene having tilted grain boundaries (Fig. 6). We expect that the length of MACC obtained from this method might be increased if graphene is elongated with a certain inclination angle normal to the line of the grain boundary since it appears that more facilitative and efficient production would be possible under an inclined elongation avoiding excessive accumulation of local stress.

These strings were sustained for a long period of time in T_i ($i = 1–3$) systems upon further elongation. From the structural analysis of this period, we found that tensile stress decreased considerably either when a string was extended chemically using carbon atoms supplied from attached graphene through bond-breaking/reforming process (Fig. 5(c) and (d)) or when a string was disconnected permanently due to elongation. Particularly, a precipitous drop in tensile stress was observed when the processes occurred simultaneously including disconnection of strings (Fig. 5(e) and (f)).

It is noted that the formation of long-lasting strings can be related to the magnitude of the misorientation angle of the tilted grain boundary, appearing at large misorientation angles. Strings were generated with the largest population and sustained largely for the T_2 grain boundary (Supplementary Movie 2) while T_i ($i = 4–6$) systems exhibited a rugged pattern

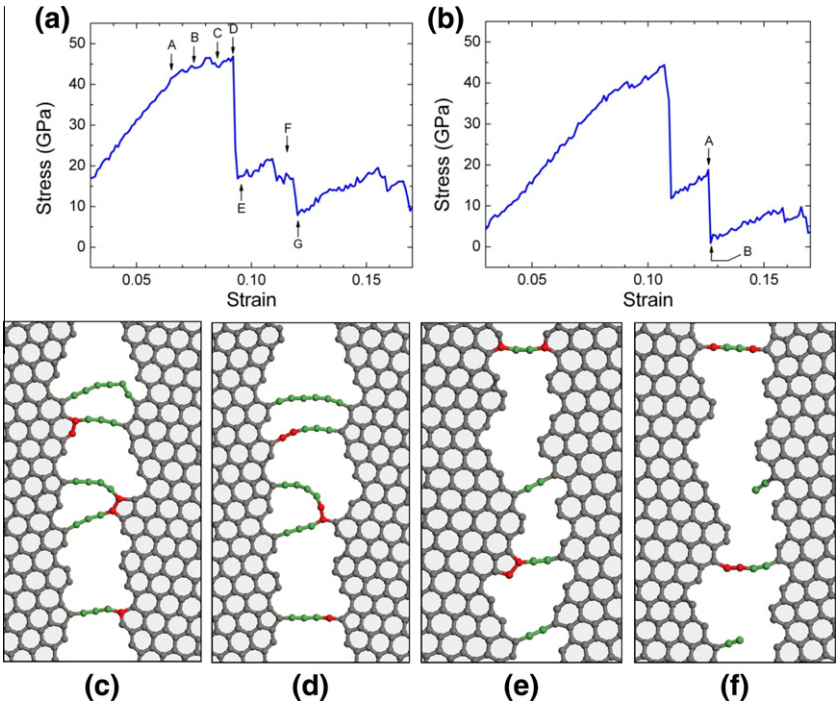

Fig. 5 – Characteristic stress–strain plots of (a) T_2 system and (b) T_3 system with indication of important stages marked with arrows. (c) and (d) The structures of T_2 system corresponding to stages of *F* and *G* in Fig. 5(a), respectively. (e) and (f) The structures of T_3 system corresponding to stages of *A* and *B* in Fig. 5 (b), respectively. Green denotes strings before chemical extension of strings and red denotes carbon atoms to be used for the chemical extension. (For interpretation of the references to color in this figure legend, the reader is referred to the web version of this article.)

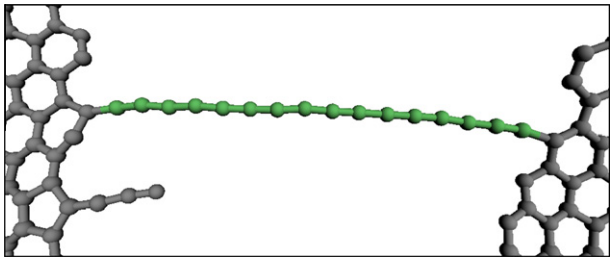

Fig. 6 – The production of monoatomic carbon chain by elongation of T_2 system in direction perpendicular to grain boundaries.

at short intervals of time. It is expected that the occurrence of prominent crack propagation in symmetric tilted grain boundaries is attributed to uneven bond strength distribution along tilted grain boundaries. Specifically, the zigzag-oriented symmetric tilt grain boundaries in graphene are constructed by aligning 5–7 defects, each of which exhibits asymmetric stress distribution. Furthermore, linkage regions between the 5 and 7 defects, composed of hexagonal bonded structures, offer additional stress non-homogeneity, and such stress distributions lead to the crack generation and propagation prior to tensile failure and the subsequent production of MMAC.

Meanwhile, a uniform distribution of bond strengths is assumed for the TZ system, as inferred from the structure of elementary defects consisting of the grain boundary and from the absence of linkage region between these defects. Hence, a pattern of complete facture was expected in this system based on the above conjectures, and it was indeed verified by our simulation (Fig. 3(d) and Supplementary Movie 3). It is interesting that an intermediate structure appearing before the creation of a one-dimensional carbon chain using controlled electron irradiation on GNR was experimentally observed to be dominated by multiple pentagons and heptagons, with the similarity to the tilted (or meandered) grain boundary [37].

3.3. *Compression perpendicular to grain boundaries*

The equilibration process frequently led to the folded structure along grain boundaries in graphene systems (see Fig. S6). The first regions of Fig. 3(a) and (c) where negligible tensile stress was required for the elongation correspond to the stages for their fold structures to be flattened. If the region of flattened structures alone is considered, the curve would be shifted to the left with an appropriate scaling, removing the first region and the resulting curve was represented in green.

As indicated by the frequent occurrence of the folded equilibrium structure, facilitative bending of graphene was observed along the tilted grain boundaries when the sheet was compressed perpendicular to grain boundaries even though it may start from its flat structure (first elongated, if necessary to be flattened). The TZ system was also folded along grain boundary under the same condition.

We observed that close relation between the positions of the folding line and grain boundary was maintained consistently during the entire compression process whereas it wan-

dered extensively and randomly over the entire region of the sheet for pristine graphene (Fig. 7 and Supplementary Movies 4 and 5). This indicates that the folding of graphene can be systematically tuned in a predictable manner using grain boundaries, and we expect it to be very significant in nanomechanic design of graphene devices. For instance, the performance of an electronic device that is tunable by the bending of graphene based on grain boundaries is conceivable.

It should be noted, herein, that grain boundaries in the systems were closely located with a separation of 24–26 Å, and the load was applied at the boundaries of a small system, which is analogous to an assembly of nano-scale compressions rather than the normal macroscopic-scale one. If the distance between grain boundaries is large, it is possible for the sheet to bend at positions other than grain boundaries or the extent of bending might be greatly weakened.

3.4. *Compression parallel to grain boundaries*

The compression (bending) perpendicular to grain boundaries does not usually require as much energy as that of elongation. We showed that this is also the same under parallel compression if the system has a flat initial structure as T6 and TZ systems (Figs. S7 and Fig. 8). For T_1 system that had initially a folded structure at the equilibrium state, however, it was found that compression applied parallel to grain boundaries required 5–6 times greater energy than that of a flat initial structure (Fig. 8(a)). This folded graphene had a sinusoidal shape from the side view where the ratio of amplitude and wavelength was around 0.186. A rapid and remarkable decrease in internal energy density (energy per unit area) occurred under a compressional strain of 0.172, and it resembles critical buckling strength that can be found in the compression of graphene attached to a substrate [41]. In addition, the slope of the curve decreased sharply from 82 to 21 meV/Å^2, indicating easier movement.

We examined the structures in detail and found that a large amount of energy was spent in drastically changing the shape of the graphene, implying a surface-shape based hindrance to the progress of the compression (Fig. 8(c)–(f) and Supplementary Movie 6). As aforementioned, this characteristic phenomenon does not appear in the T_6 system that has a flat structure initially, and it is supposed that a fold that was created along the grain boundary should play a critical role as an intrinsic reinforcement in the phenomenon. To examine this point more fully, the structure of the T_1 system was flattened by elongating its equilibrium structure under a strain of 0.075 perpendicular to grain boundaries, and it was subsequently compressed parallel to them. Its energy density variation on compression was quite similar to that of the T_6 system (Figs. 8(a) and S7), and the slope of the curve was much smaller than that of the initially folded structure. In addition, conversely, a flat equilibrium structure of the TZ system was folded along its grain boundaries by perpendicular compression to a strain of 0.075 resulting in the wavelike folded structure where the ratio of amplitude and wavelength

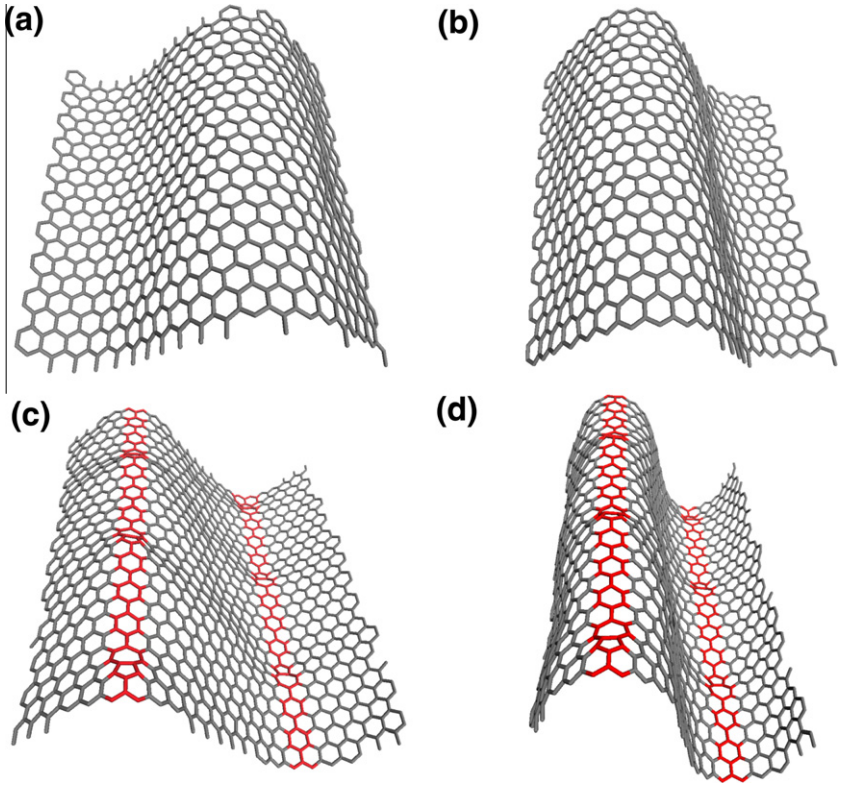

Fig. 7 – The structural variation of graphenes under compression perpendicular to grain boundaries. (a) and (b) The structures of PR system at compressional strain of 0.214 and 0.28, respectively. (c) and (d) The structures of T_4 system at compressional strain of 0.2 and 0.4, respectively. Grain boundaries are highlighted in red for clarity. (For interpretation of the references to color in this figure legend, the reader is referred to the web version of this article.)

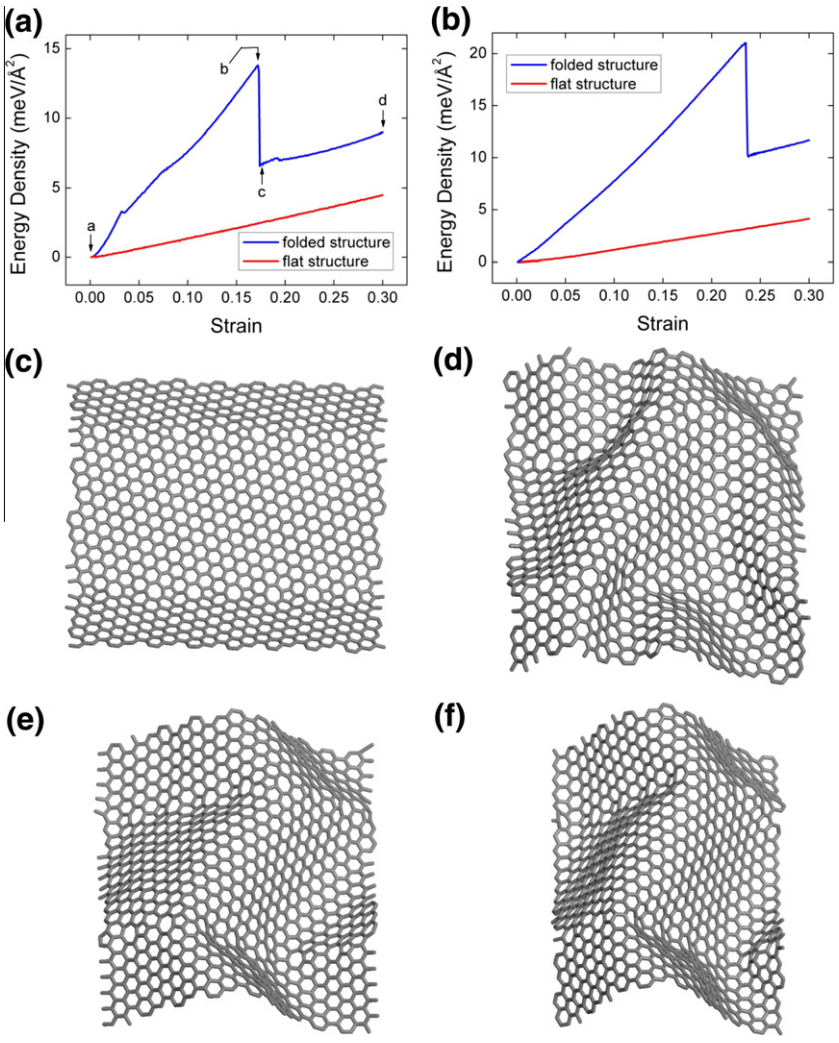

Fig. 8 – The variation of energy density under compression parallel to grain boundaries for the folded and flat structures of (a) T_1 system and (b) TZ system. (c)–(f) The structures of T_1 system corresponding to stages of *A–D* in Fig. 8(a), respectively.

was 0.190. Then, the plots of energy density vs. strain were obtained under compression parallel to grain boundaries for the flat and folded structures of the TZ system, respectively. They showed result consistent with the T_1 system (Fig. 8).

4. Conclusion

We illustrated that the existence of grain boundaries in graphene generated many intriguing variations of mechanical properties by indicating their crucial significance in nanomechanics and nanoelectronics. Especially, we found that the tilted grain boundaries exhibit very unique tensile behavior in contrast to pristine graphene and non-tilted grain boundaries, accompanied by a feasible production of monoatomic chains that are extremely difficult to synthesize and extract in practice. It is inferred that the presence of a prominent non-homogeneity in stress distribution along a tilted grain boundary, sufficient stress relaxations achieved during the crack propagation, and strong yet very flexible properties of graphene played critical roles in the occurrence of the phenomenon. To make better technological improvements in graphene engineering, we propose that further investigations should be performed on the characteristics of graphene grain boundaries, including multiscale modeling to fully understand properties of large-scale polycrystalline graphene. Although our analysis was based on an isothermal environment, it is expected that these findings on the mechanical response of grain boundaries reported here will contribute significantly in developing novel design criteria for grain boundary-based graphene devices in conjunction with applications of thermomechanical response.

Acknowledgement

This work was supported by the World Class University program of KOSEF (Grant No. R32-2008-000-10124-0).

Appendix A. Supplementary data

Supplementary data associated with this article can be found, in the online version, at http://dx.doi.org/10.1016/j.carbon.2012.03.044.

REFERENCES

[1] Chen JH, Jang C, Xiao S, Ishigami M, Fuhrer MS. Intrinsic and extrinsic performance limits of graphene devices on SiO_2. Nat Nanotechnol 2008;3:206–9.
[2] Bolotin KI, Sikes KJ, Jiang Z, Klima M, Fudenberg G, Hone J, et al. Ultrahigh electron mobility in suspended graphene. Solid State Commun 2008;146:351–5.
[3] Balandin AA, Ghosh S, Bao W, Calizo I, Teweldebrhan D, Miao F, et al. Superior thermal conductivity of single-layer graphene. Nano Lett 2008;8(3):902–7.
[4] Seol JH, Jo I, Moore AL, Lindsay L, Aitken ZH, Pettes MT, et al. Two-dimensional phonon transport in supported graphene. Science 2010;328:213–6.
[5] Lee C, Wei X, Kysar JW, Hone J. Measurement of the elastic properties and intrinsic strength of monolayer graphene. Science 2008;321:385–8.
[6] Zhao H, Min K, Aluru NR. Size and chirality dependent elastic properties of graphene nanoribbons under uniaxial tension. Nano Lett 2009;9(8):3012–5.
[7] Liu F, Ming PM, Li J. Ab initio calculation of ideal strength and phonon instability of graphene under tension. Phys Rev B 2007;76:064120.
[8] Banhart F, Kotakoski J, Krasheninnikov AV. Structural defects in graphene. ACS Nano 2011;5(1):26–41.
[9] Li X, Cai W, An J, Kim S, Nah J, Yang D, et al. Large-area synthesis of high-quality and uniform graphene films on copper foils. Science 2009;324:1312–4.
[10] Bae S, Kim H, Lee Y, Xu X, Park JS, Zheng Y, et al. Roll-to-roll production of 30-inch graphene films for transparent electrodes. Nat Nanotechnol 2010;5:574–8.
[11] Coraux J, N'Diaye AT, Engler M, Busse C, Wall D, Buckanie N, et al. Growth of graphene on Ir(111). New J Phys 2009;11:023006.
[12] Miller DL, Kubista KD, Rutter GM, Ruan M, Heer WAD, First PN, et al. Observing the quantization of zero mass carriers in graphene. Science 2009;324:924–7.
[13] Loginova E, Nie S, Thurmer K, Bartelt NC, McCarty KF. Defects of graphene on Ir(111): rotational domains and ridges. Phys Rev B 2009;80:085430.
[14] Park HJ, Meyer J, Roth S, Skákalová V. Growth and properties of few-layer graphene prepared by chemical vapor deposition. Carbon 2010;48:1088–94.
[15] Stone AJ, Wales DJ. Theoretical studies of icosahedral C60 and some related species. Chem Phys Lett 1986; 128(5–6):501–3.
[16] Thrower PA. The study of defects in graphite by transmission electron microscopy. Chem Phys Carbon 1969;5:217–320.
[17] Gass MH, Bangert U, Bleloch AL, Wang P, Nair RR, Geim AK. Free-standing graphene at atomic resolution. Nat Nanotechnol 2008;3:676–81.
[18] Meyer JC, Kisielowski C, Erni R, Rossell MD, Crommie MF, Zettl A. Direct imaging of lattice atoms and topological defects in graphene membranes. Nano Lett 2008;8(11): 3582–6.
[19] Krasheninnikov AV, Lehtinen PO, Foster AS, Pyykko P, Nieminen RM. Embedding transition-metal atoms in graphene: structure, bonding, and magnetism. Phys Rev Lett 2009;102:126807.
[20] Malola S, Hakkinen H, Koskinen P. Structural, chemical, and dynamical trends in graphene grain boundaries. Phys Rev B 2010;81:165447.
[21] Yazyev OV, Louie SG. Topological defects in graphene: dislocations and grain boundaries. Phys Rev B 2010;81:195420.
[22] Lahiri J, Lin Y, Bozkurt P, Oleynik II, Batzill M. An extended defect in graphene as a metallic wire. Nat Nanotechnol 2010;5:326–9.
[23] Yazyev OV, Louie SG. Electronic transport in polycrystalline graphene. Nat Mater 2010;9:806–9.
[24] Liu Y, Yakobson BI. Cones, pringles, and grain boundary landscapes in graphene topology. Nano Lett 2010;10:2178–83.
[25] Grantab R, Shenoy VB, Ruoff RS. Anomalous strength characteristics of tilt grain boundaries in graphene. Science 2010;330:946–8.
[26] Huang PY, Ruiz-Vargas CS, van der Zande AM, Whitney WS, Levendorf MP, Kevek JW, et al. Grains and grain boundaries in single-layer graphene atomic patchwork quilts. Nature 2011;469:389–93.
[27] Zhao H, Aluru NR. Temperature and strain-rate dependent fracture strength of graphene. J Appl Phys 2010;108:064321.
[28] Pei QX, Zhang YW, Shenoy VB. A molecular dynamics study of the mechanical properties of hydrogen functionalized graphene. Carbon 2010;48:898–904.
[29] Delley B. From molecules to solids with the DMol3 approach. J Chem Phys 2000;113(18):7756–64.
[30] Plimpton S. Fast parallel algorithms for short-range molecular dynamics. J Comput Phys 1995;117:1–19.
[31] Stuart SJ, Tutein AB, Harrison JA. A reactive potential for hydrocarbons with intermolecular interactions. J Chem Phys 2000;112(14):6472–86.
[32] Tuckerman ME, Mundy CJ, Balasubramanian S, Klein ML. Modified nonequilibrium molecular dynamics for fluid flows with energy conservation. J Chem Phys 1997;106(13):5615–21.
[33] Liu Y, Jones RO, Zhao XL, Ando Y. Carbon species confined inside carbon nanotubes: a density functional study. Phys Rev B 2003;68:125413.
[34] Zhao XL, Ando Y, Liu Y, Jinno M, Suzuki T. Carbon nanowire made of a long linear carbon chain inserted inside a multiwalled carbon nanotube. Phys Rev Lett 2003;90(18):187401.
[35] Qi Z, Zhao F, Zhou X, Sun Z, Park HS, Wu H. A molecular simulation analysis of producing monatomic carbon chains by stretching ultranarrow graphene nanoribbons. Nanotechnol 2010;21:265702.
[36] Jin C, Lan H, Suenaga K, Iijima S. Deriving carbon atomic chains from graphene. Phys Rev Lett 2009;102:205501.
[37] Chuvilin A, Meyer JC, Algara-Siller G, Kaiser U. From graphene constrictions to single carbon chains. New J Phys 2009;11:083019.
[38] Akdim B, Pachter R. Switching behavior of carbon chains bridging graphene nanoribbons: effects of uniaxial strain. ACS Nano 2011;5(3):1769–74.
[39] Heimann RB, Evsyukov RB, Kavan L. Carbyne and carbynoid structures. Berlin: Springer; 1999.
[40] Cataldo F. Polyynes: synthesis, properties and applications. Boca Raton; 2005.
[41] Frank O, Tsoukleri G, Parthenios J, Papagelis K, Riaz I, Jalil R, et al. Compression behavior of single-layer graphenes. ACS Nano 2010;4(6):3131–8.